京都大学防災研究所年報　第44号 B-1　平成13年4月
Annuals of Disas, Prev. Res. Inst., Kyoto Univ., No.44 B-1, 2001

Failure and Triggering Mechanism Analysis of the Bitchu-Matsuyama Castle Rock Using Distinct Element Method

GREIF Vladimir, SASSA Kyoji, FUKUOKA Hiroshi

Synopsis

In this paper a rock slope failure of Bitchu-Matsuyama castle rock located near Takahashi city in the central part of Okayama prefecture is presented. Rock mass creep movement, which mechanism and triggering factors are studied here, endangers the castle, which walls are suffering damage and need to be repaired. In order to find the reason of the damage various triggering factors such as weathering progress, slope-toe erosion (toe sliding) and a special phenomena for this site – wind tree action are simulated using distinct element method (DEM), namely UDEC (Universal Distinct Element Code) as one of the numerical modeling codes. The joint shear displacements of several points are observed in the model as key factors for result comparison. Further a failure analysis of rock slope is carried out in order to find out the future behavior of the rock slope and optimize the design of monitoring system, which is in process of installation.

Keywords: DEM; UDEC; rock slope; failure mechanism

1. Introduction

Historical heritage is undoubtedly one of the most important treasures of every nation and culture and is therefore responsible for their maintenance and preservation. From the factors endangering mainly the old castles build on the rock substrate are the most common various kinds of rock movements. Prior to maintenance or preservation works a type and size of the movement must be defined. These movements are usually determined mainly by the presence of discontinuities, which divides the rock mass into separate blocks. The determination of such blocky rock mass behavior is quite difficult task. One possibility is to use numerical modeling specifically distinct element modeling as one of the numerical methods applicable for the assessment of blocky system behavior. In this paper a study of such jointed rock mass, which also serves as foundation bedrock for Bitchu-Matsuyama castle dating back into the 13-th century. The rock mass creep movement, which mechanism and triggering factors are at present not clear, endangers the castle, which walls are suffering moderate damage and need to be repaired. In order to find the reason of the damage various triggering factors including weathering and its progress towards the slope along the joints, slope-toe erosion (toe sliding) and a special phenomena in this site – wind tree action causing loosening of blocks due to the oscillation transferred to the joints by roots are simulated using distinct element method, namely UDEC numerical modeling code. The changes in joint shear displacement are observed as key actors for result comparison.

2. Geological settings and structural analysis.

Bitchu-Matsuyama castle is located in the central part of Okayama prefecture near the Takahashi city on rather steep slope of Mt. Gagyu at 430 meters above the sea level. The bedrock of Bitchu Matsuyama Castle is formed by granitic rocks being a member of Hiroshima intrusives, petrographic province of Sany´o belt reaching the thickness several hundreds of meters.

Fig. 1: Map of Japan showing the location of Bitchu-Matsuyama Castle

From the petrological point of view coarse to medium grained hornblende-biotite adamellite (personal communication Prof. Yokoyama Shunji) granites prevail. Important feature of the granitic rocks in castle rock of Bitchu Matsuyama is an expressive loosening of rock slope upon which part of defense walls stands. The loosening as a result of relative dense net of discontinuity appearance may be the result of a several different reasons. Among the most important belong:

1. primary cooling joints,
2. tectonic joints controlled by regional tectonic stresses during the latest cooling stage of granitic magma,
3. joints controlled by regional fault tectonics

Differential geotectonic development of the area in the late Pliocene and Quaternary resulted in a mosaic of different structural - morphological elements as a result of uplift and the following horizontal stress relief. Subsequently the existing faults (NNW-SSE and approximately N-S directions developed. To the tectonic predisposition of the area corresponds also the orientation of the adjacent valleys surrounding the Mt. Gagyu. As a result of stress release, young open tension cracks occurred and the weathering processes proceeded relatively rapidly.

The discontinuity system dominantly contributed to the morphostructural division of the rock structure on which the Castle is founded and resulted in expressive cliff morphology, which developed in SE part of the Castle rock, nearby the access road to the castle immediately below the SE outer defense walls. The temporal investigation of the 35 m rock face proved that the granitic rock body is massive, disturbed by a series of discontinuities of different origin. According the structural analysis, three major discontinuity systems can be found (Fig. 2):

F_1 = 68-90°/65-80° (dip direction/dip) with the direction NNW to SSE and dipping to NNE;

F_2 = 130-160°/80-88° with the direction NE-SW and dipping to SE and

F_3 = 185-220°/75-88° with the direction NNE-SSW and dipping to SW. A close connection exists between the orientation of fault system forming the valley of Takahashi River passing Takahashi city with the joint systems F_1 and its tributary catching the small river north from Takahashi city which corresponds to the system F_2 (slightly also to F_3).

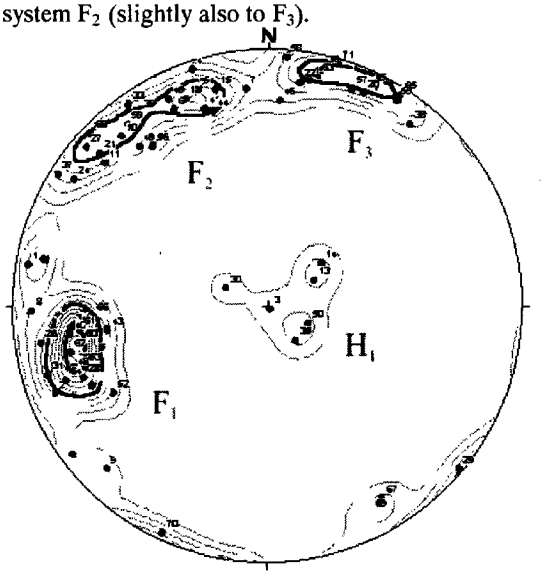

Fig. 2: Results of structural analysis of joints with three almost vertical sets F_1 through F_3 and sub-horizontal set H_1. Schmidt projection lower hemisphere

The discontinuities of horizontal or sub horizontal orientation H_1, which are of not clarified origin are outlined with disperse (scattered) orientations but relatively uniform dip reaching 15-20°.

The spacing between discontinuities is generally widely spaced (60-200 cm) to very widely spaced (> 2 m), roughness of the discontinuities is rather planar and smooth, aperture differs from place to place and ranges from narrow (2-6 mm) to moderately wide (20-60 mm) according to the IAEG rock and soil classification (Matula, 1981).

3. DEM model

The distinct element method introduced in 1971 by Cundall (Cundall, 1971) has found many applications in study of jointed rock masses. Different failure mechanisms were studied in both natural and artificial rock slopes. The usage of DEM attracted attention of engineers as well in problematic of slope design (Sjöberg, 1999). In the field of natural slope failure mechanism investigation the usage of DEM was focused mainly on toppling failure mechanism

(Pritchard and Savigny, 1990; Deangeli and Ferrero, 2000; Pritchard and Savigny, 1991), problems of rock cliff failure (Allison and Kimber, 1998) and rock slope stability problems (Zhang et al., 1997; Benko et al., 1994).

The essential feature of the distinct element method is its ability to model the arbitrary motion of each block with respect to any other. Block may be rigid or deformable. Because most slope stability problems involve stresses that are relatively low compared with the block strength and deformability, the blocks are usually considered rigid. The distinct element method is based on a dynamic algorithm that solves the equations of motion of the block system by an explicit finite difference method. For the analysis a distinct element code called UDEC was used. In this code the displacement on the contact is governed by the Coulomb's frictional law, where the movement on the joint is permitted when the tangential force at a contact exceeds a critical value, F_S, defined by:

$$|F_s| = C + F_n \tan \phi \qquad \text{Eq. 1}$$

where C is the cohesion, and ϕ is the basic joint friction angle. Before reaching the value of F_s the contacts behave as elastic according to:

$$F_n = k_n u_n \qquad \text{Eq. 2}$$

where F_n = normal force at the contact,
k_n = normal stiffness at a point, and
u_n = total normal penetration

and

$$\Delta F_s = k_s \Delta u_s \qquad \text{Eq. 3}$$

where ΔF_s = change in shear force,
k_s = shear stiffness at a point, and
Δu_s = incremental shear displacement.

The motion law is based on the Newton's second law of motion, which expressed in finite difference form becomes:

$$\dot{u}_i^{(t+\Delta t/2)} = \dot{u}_i^{(t-\Delta t/2)} + \left(\frac{\sum F_i^{(t)}}{m} + g_i \right) \Delta t \qquad \text{Eq. 4}$$

where $\dot{u}_i$ = velocity components of block centroid
g_i =gravitational acceleration components
ΣF_i = sum of the forces acting on the block
m = block mass, and
Δt = timestep

The motion laws and joint constitutive relations are applied at each timestep. The integration of the motion law provides the new block position and joints displacement increments. Blocks are assumed to interact at discrete points referred to as "contacts" (Fairhurst C. and Lorig J. in Sharma et al., 1999). The calculation cycle for rigid and deformable blocks are illustrated in Fig. 3.

The model geometry was created from the digital photograph oriented in direction of potential movement WSW-ENE and direction of joints were represented using automatic joint generator implemented into UDEC. The initial deformational and mechanical parameters of rock namely Yong's modulus, Poisson ratio, density and tensile strength necessary for the model were found out from uniaxial compression tests of samples taken from the rock.

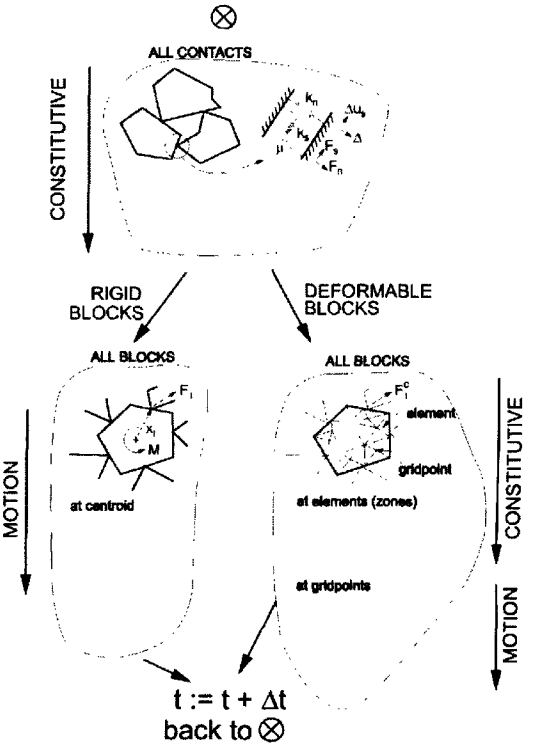

Fig. 3 Process of new block calculation for rigid and deformable blocks

Some values as intact rock friction angle and joint fiction angles were assumed from the properties of the similar types of rocks (Tab.1). Values of normal and shear joint stiffnesses were calculated from Eq.5 and Eq.6 respectively with Young's modulus of rock mass assessed to be 18 GPa and joint spacing 5m.

$$k_n = \frac{E_m E_r}{s(E_r - E_m)} \qquad \text{Eq. 5}$$

$$k_s = \frac{G_m G_r}{s(G_r - G_m)} \qquad \text{Eq. 6}$$

$$G_m = \frac{E_m}{2(1+\nu)} \qquad \text{Eq. 7}$$

where: k_n and k_s are joint normal and shear stiffnesses respectively, E_r is intact rock Young's modulus, G_r is intact rock shear modulus, E_m is rock mass Young's modulus G_m is rock mass shear modulus, s is joint spacing and ν is Poisson's ratio. Value of joint

		Triggering factor analysis	Failure mechanism analysis
Material property	Rock	Joints	Joints
Young's modulus E (GPa)	21		
Poisson ratio ν	0.144		
Density ρ (kg/m^3)	2,600		
Tensile strength (MPa)	10		
Friction angle ϕ (°)	48-38	32-16	48-28
Normal stiffness K_n (GPa/m)		23	50
Shear stiffness K_s (GPa/m)		10	10
Joint roughness parameter (m)		$1x10^{-2}$	

Table 1 Mechanical and deformational properties of rocks and joints used in UDEC

roughness parameter was determined from field observation.

For the purpose of triggering factor analysis the continuously yielding model of joint was chosen for representation of joint behavior, which is suitable for simulation of progressive damage of joints under shear and provides continuous hysteretic damping for dynamic simulations (Itasca, 1999). The rock mass was considered to be deformable with Mohr-Coulomb plasticity. The analysis of movement mechanism was performed on the modified model, using cell-mapping logic useful for the detection of larger relative displacements of blocks, which reduced the calculation time necessary for the simulation. The normal joint stiffness was increased approximately two times to the vale 50 GPa/m to avoid large block overlaps. The boundary conditions were applied as in Fig.4 the left boundary was restricted from motion in X direction and the bottom boundary was immobilized in the Y direction. After applying gravitational acceleration the model was brought to equilibrium. From this point all other simulations were started.

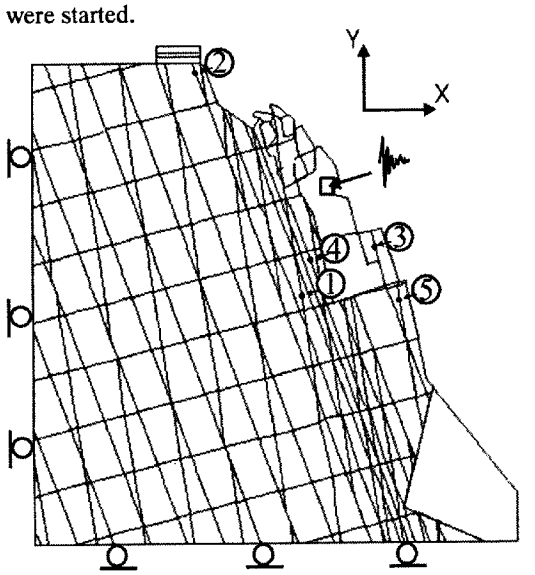

Fig. 4 Model of the studied rock slope showing the boundary conditions, points of joint displacement measurement ①-⑤ and place of applied cyclic loading

4. Triggering factor analysis

For the analysis of possible triggering factors of movement a continuously yielding model of joints was chosen. Four potential triggering factors were studied, weathering progress, toe slide, wind tree action and combination of weathering and toe slide. Initial geometry in Fig. 4 was the same for all studied factors.

4.1 Weathering progress

The simulation of weathering progressing along the joints towards the rock mass was carried out by decreasing the joint friction angle in steps as other joint properties proved to have lower effect on the resulting movements.

After applying gravitational acceleration the system was brought to equilibrium, which was the initial condition for applying of weathering simulation. As could be seen from Fig.5 the weathering was simulated in steps where to a region of depth 2 meters

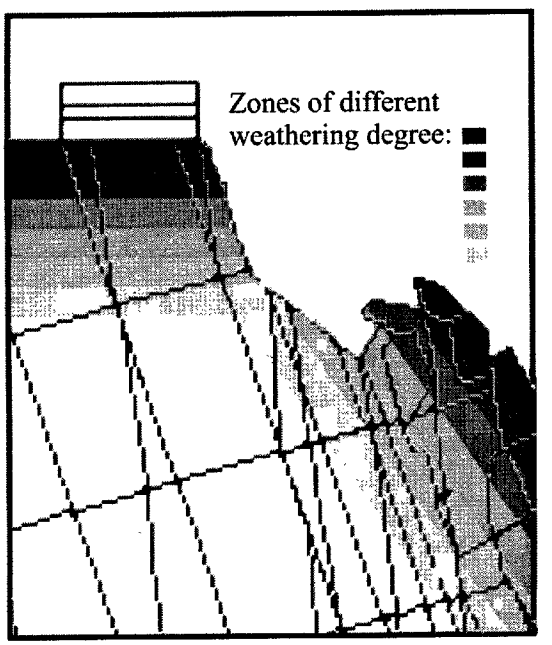

Fig. 5 Example of weathering simulation. Close-up of the model – darker colors represent higher degree of weathering (smaller joint friction angle)

was always assigned same joint friction angle 2 degrees lower than the previous. This procedure was carried out in cycles where the region immediately below slope surface was assigned joint friction angle 32° and the rest of the slope remained unaltered. In the next cycle the region with joint friction angle 32° was changed to 30° and the region with ϕ = 32° was moved 2m deeper to the slope. After each cycle the slope was brought to equilibrium. Using this method it was possible effectively simulate the propagation of weathering towards the slope. The range of assigned joint friction angles was from 32° to 16° with already mentioned step of 2°. The final depth of weathering effect was 18 m where the deepest region was assigned joint friction angle 32° whereas the surface region value 16°.

4.2 Toe slide

Second triggering factor was simulated after bringing the system to equilibrium, the same state as in the previous case. The toe erosion was modeled by removing a big block from the toe region of the slope, which caused release of stress in the region immediately above the toe erosion area.

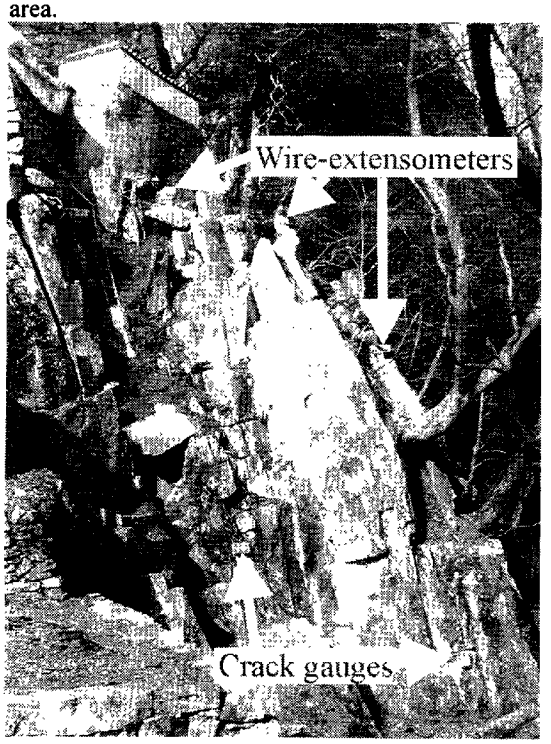

Fig. 6 Photograph of the studied rock slope with installed monitoring devices

There were several points in the model chosen mainly on the dominant joints observable in the real condition as well in order to monitor corresponding joint shear displacements. There were 5 points chosen as could be seen in Fig.4 (①-⑤), one in the upper slope, 2 in the region of strongly jointed rock and 2 in the area near surface.

4.3 Wind tree action

Many trees are found to be growing in the joints and thus influence the stability of rock slopes. Since this area is protected, the trees cannot be cut out. This fact was the stimulus for dealing with this phenomenon. The wind is causing the swinging of the tree and this oscillation is transferred to the rock joints through the roots growing there. The roots also generate a pressure on the joints causing the opening of the crack. In this study only the momentum of the wind tree action transferred to rock was studied. This process was modeled numerically by applying cyclic shear stress in the form of sinusoidal wave with frequency 2Hz and amplitude 425 kPa in the big block, where a rather big tree is growing. The amplitude was assessed from the

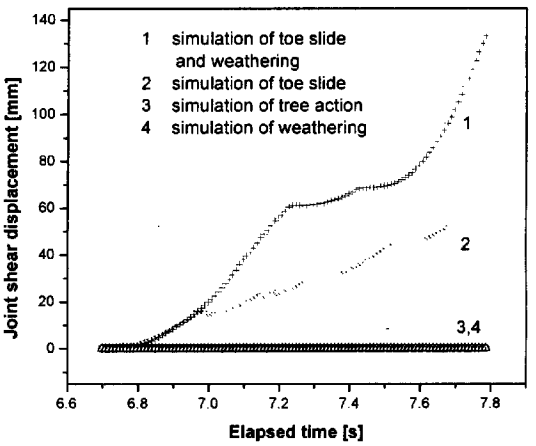

Fig. 7 Joint shear displacements for various triggering factors recorded in point No. 3

tree properties, namely weight and height, the active contact area between roots and rock was assessed to be 1m.

4.4 Results

In order to keep maximal accuracy of numerical model the chosen timestep was very small $1x10^{-4}$s, which allowed compare various triggering factors of movement. Figure 7 shows the comparison between four factors possibly causing the movement recorded in point No. 3. It is clear that weathering and tree action doesn't cause any shear displacement, but the toe slide is the most probable cause of the movement. However the weathering is the accelerating factor for movements if is applied together with toe block removal. This confirms the theory which assumes the toe slide to be the triggering factor of the rock instability, based on the presence of tension crack in the upper part of the rock slide right under the fortification fence.

5. Failure mechanism analysis

Considering the previous results of triggering factor analysis the toe slide seemed to be the most dangerous factor of sliding. In the further investigation it was necessary to find out the mechanism of the rockslide in order to be able predict the future behavior of the rock slope and optimize the monitoring system installation to find the best solution for stabilizing the slope. Therefore it was necessary to achieve longer simulation time and exaggerate the movement to be able recognize the mechanism of rock slope failure. This was done in several ways. First, the contact detection was changed to cell-mapping logic, which should secure the ability of contact tracing also with awaited larger displacements. Than the blocks were changed from the deformable to rigid, because there was no big difference between resulting paths of blocks and since there was no calculation necessary for the block deformability it reduced the calculation time. The timestep was increased to the value of $1x10^{-2}$ s, which decreased the calculation time but increased the errors as well. But for the purpose of finding out the mechanism of failure the generated errors could be neglected. Finally the joint friction angle was decreased to 5°. The triggering factor for movement was the toe slide simulated by removing one block from the toe area of slope. During the simulation three factors were monitored, namely maximal unbalanced force, joint shear displacement at five points in the slope and each 1000 calculation steps a snapshot of the model was taken in order to reveal the mechanism of failure.

5.1 Results

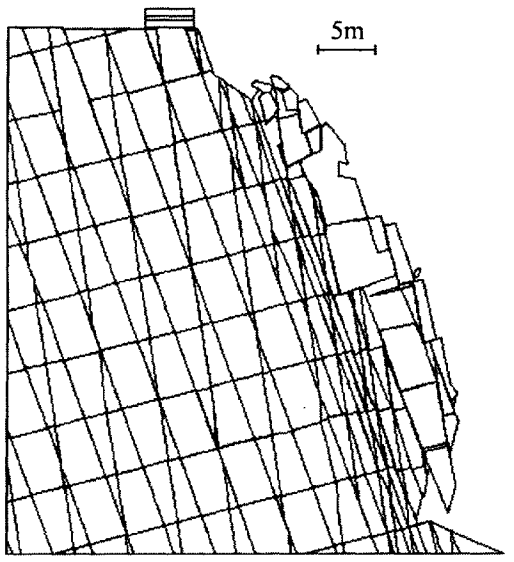

Fig. 8 Failure mechanism simulation – model after 18,000 steps

From the history of maximal unbalanced force, which is an indicator of stability of the blocky system, was clear that the system is not in steady state.

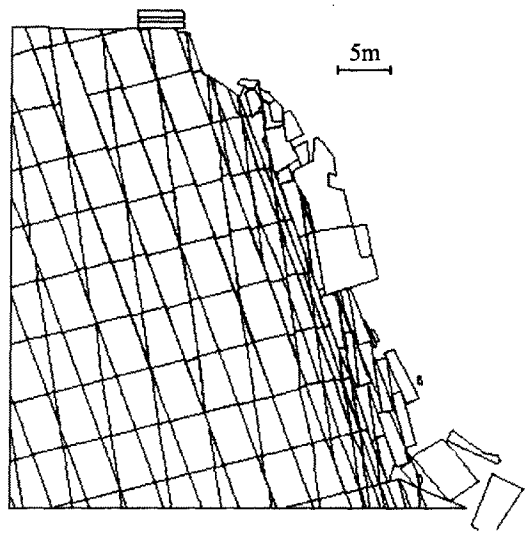

Fig. 9 Failure mechanism simulation – model after 150,000 steps

By observing the simulation progress in the recorded snapshots the movement could be divided into two phases. In the first the block were moving along planar sliding surfaces dipping in the same direction with slope face Fig.8. More complex shear surface developed in the region of heavily jointed rock behind the big central block.

In the second phase the central block was subjected to toppling failure and following fall as seen in Fig.10. From the sequence is clear the damage caused to the one of the defense walls standing on the top of the slope.

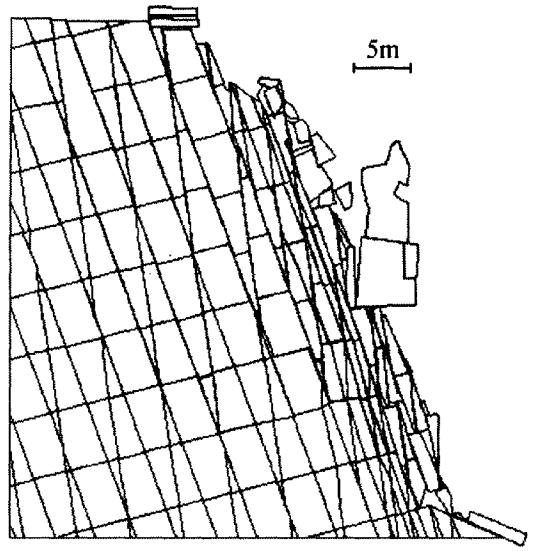

Fig. 10 Failure mechanism simulation – model after 322,000 steps

This type of failure is most likely the causing factor of failure of the wall, which is clear from the damage of

the masonry foundation of the wall damaged by tension failure Fig.12.

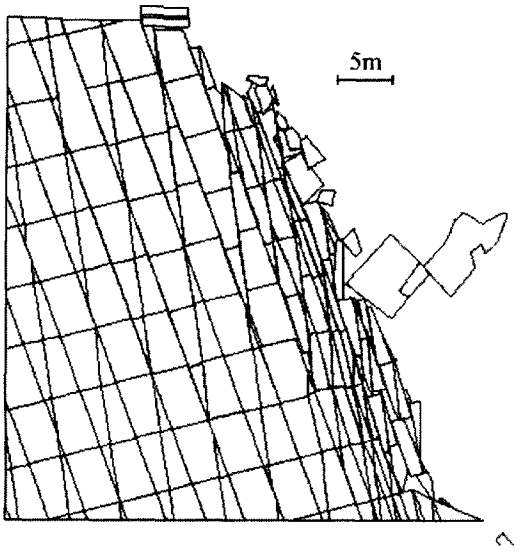

Fig. 11 Failure mechanism simulation – model after 360,000 steps

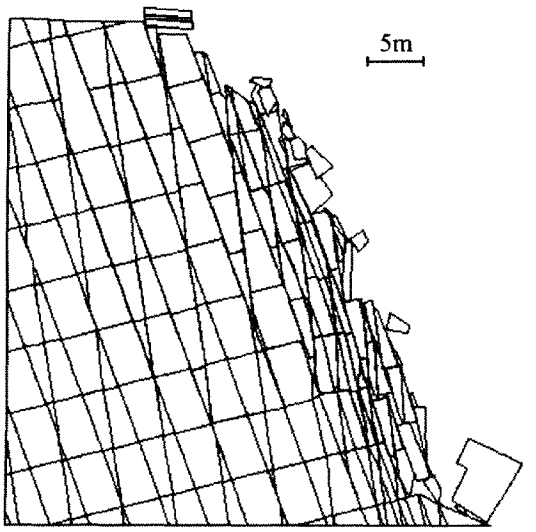

Fig. 12 Failure mechanism simulation – model after 400,000 steps

6. Conclusions and discussion

The distinct element method represented by the computer code UDEC showed good ability to recognize the triggering factors of rock slope movements and also the mechanism of failure. In the triggering mechanism analysis the most endangering factor of the castle fortification proved to be the toe slide, which occurred under the main rock body. The weathering progressing along the joints greatly accelerated the shear displacements on joints. This indicates that the triggering factor of movements must be with high probability dynamic. Despite the fact that the duration of simulation was short the differences was clearly showed. The wind tree action haven't had an effect on the joint displacement, however the place of applied shear stress was in the big block (Fig. 4), whereas the roots are growing mainly in the joints. This was mainly due to the inability of proper interpretation of root-rock contact in two-dimensional UDEC. Nevertheless the wind tree action has mainly local character, but in special cases could contribute to instability of whole rock slope.

Using the results of the simulation and in order to be able compare the UDEC simulation with reality a monitoring system composed of crack gauges and extensometers (Fig. 6) was installed at the end of year 2000. Movements up to 1.2 mm were recorded since the beginning of this year. However the period is not satisfactory for decision of rates of movement or comparison with simulation, it shows that the rock slope is not stable and is in constant creep movement.

Acknowledgments

The research was carried out in cooperation with the Takahashi city Board of Education of Okayama Prefecture. Mr. K. Osafune (superintendent of schools), Mr. M. Kunida and Mr. H. Mori are acknowledged for their support and cooperation. Authors want to thank to Assoc. Prof. T. Kamai and Mr. Y. Tamari for their extensive help in field investigations. Special thanks go to Mr. H. Mori for his mediatory work and his announcements without which the field study would not be possible.

References:

Allison, R. J., Kimber, O. G. (1998): Modelling Failure Mechanisms to Explain Rock Slope Change Along the Isle of Purbeck Coast, UK. Earth Surface Processes and Landforms, 23, pp. 731-750

Benko, B., Stead, D., Malgot, J. (1994): Numerical analysis of block movements as a slope failure mechanism, 7th International IAEG Congress, Balkema Rotterdam, pp.4729-4735

Chuhan, Z., Pekau, O. A., Feng, J., Guanglun, W. (1997): Application of distinct element method in dynamic analysis of high rock slopes and blocky structures, Soil Dynamics and Earthquake Engineering, 16, pp. 385-394

Cundall, P. A. (1971): A Computer Model for Simulating Progressive Large Scale Movements in Blocky Rock Systems, Proccedings of the Symposium of the International Society of Rock Mechanics (Nancy, France,1971), Vol. 1, pp.132-150

Deangeli, C., Ferrero, A. M. (2000): Rock Mechanics Studies to Analyse Toppling Failure, Landslides in

research, theory and practice, Thomas Telford, London
Itasca, (1990): Udec version 3.10 – User manual, Itasca Consulting Group Inc., Minneapolis, Minnesota
Matula, M. (1981): Rock and Soil Description and Classification for Engineering Geological Mapping Report by the IAEG Commission on Engineering Geological Mapping, Bulletin of the International Association of Engineering Geology, 24, pp.235-274
Pritchard, M. A., Savigny, K. W. (1990): Numerical modelling of toppling, Canadian Geotechnical Journal 27, pp. 823-834
Pritchard, M. A., Savigny, K. W. (1991): The Heather Hill landslide: an example of large scale toppling failure in a natural slope, Canadian Geotechnical Journal 28, pp. 410-422
Sharma, V. M., Saxena, K. R., Woods, R. D. (1999): Distinct Element Modelling in Geomechanics, Balkema Rotterdam, pp.220
Sjöberg, J. (1999): Analysis of Large Scale Rock Slopes, Doctoral thesis Luleå University of Technology Sweden, pp.682

要旨

岡山県中央部の高梁市にある備中松山城の大手門岩盤においては落石，クラックの進行，クリープ挙動が現れ，対策工の必要性が指摘されている．この岩盤斜面について崩壊誘因と崩壊メカニズムについて検討した．風化の進行，斜面末端の地すべり運動，および風によるクラックに貫入した樹根による揺さぶり等の諸要因による影響を解決するために離散要素法(DEM)，特にUDECプログラムを用い，節理面に沿ったせん断変位に注目してシミュレーションを行った．さらに現在設置中の監視システムの最適化のための岩盤斜面の今後の挙動予測を行った．

キーワード： 離散要素法(DEM)，UDEC，岩盤斜面，崩壊メカニズム